Article

Tuning the Catalytic Activity of Synthetic Enzyme KE15 with DNA

Yi Zheng and Valerie Vaissier Welborn*

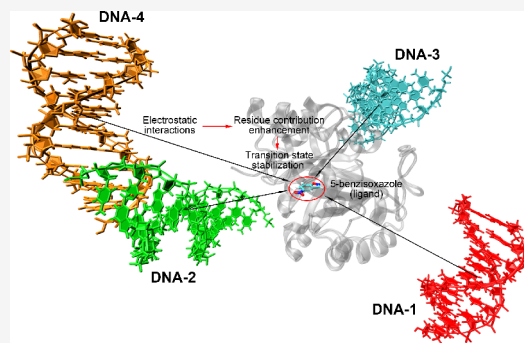Read Online

ACCESS | Metrics & More | Article Recommendations | SI Supporting Information

ABSTRACT: Efficiency improvement of synthetic enzymes through scaffold modifications suffers from limitations in terms of effectiveness, cost, and potential devastating consequences for protein structural stability. Here, we propose an alternative to scaffold modification, within electrostatic preorganization theory, where the enzyme's greater environment is designed to support the evolution of the reaction in the active site. We demonstrate the feasibility of such an approach by placing a (polar) DNA fragment in the surroundings of the Kemp eliminase enzyme KE15 (structure from Houk's group) and computing the resulting change in catalytic activity. We find that the introduction of a DNA fragment magnifies the contribution of protein residues to the stabilization of the transition state, estimated from electric field calculations with polarizable molecular dynamics. Our randomly generated test systems reveal a 2.0 kcal/mol reduction in activation energy, suggesting that even more significant catalytic improvements could be made by optimizing DNA size, sequence, and orientation with respect to the enzyme, validating our approach.

INTRODUCTION

Synthetic enzymes, engineered to catalyze reactions not found in nature, have the potential to transform the chemical industry, providing they exhibit high efficiency.[1−3] Although several approaches have been developed to design synthetic enzymes, computational methods stand out for their relatively low labor and time demand.[4−6] However, thus far, rate accelerations from computationally designed enzymes are orders of magnitude below those of their natural counterparts.[7−10]

Several studies have attributed this poor efficiency to the lack of scaffold optimization for function, a strong limitation in the computational enzyme design process.[11−13] The family of Kemp eliminases computationally designed by Baker and co-workers has been extensively studied, both experimentally and theoretically, which makes them a paradigm of synthetic enzymes.[14−19] For Kemp eliminases and other synthetic enzymes, the active site was crafted first to stabilize the reaction transition state,[20−22] thereby mimicking the process by which natural enzymes catalyze reactions.[23,24] Then, a search for existing protein scaffolds was performed, aiming to accommodate the theoretical active site based on ligand affinity and protein stability.[4,25,26] This implies that these scaffolds have limited contribution to the stabilization of the transition state,[27−30] in contrast with natural enzyme scaffolds that actively contribute to the evolution of the reaction in the active site.[31]

To address this issue, experimental methods including laboratory directed evolution (LDE) were employed to improve computational enzyme designs, yielding mutations within the protein scaffold.[15,32−36] Despite notable success in enhancing the performance of some synthetic enzymes,[33,37,38] LDE-based improvements are not guaranteed, which makes its intensive cost a difficult trade-off.[39,40] Further, modifications of protein scaffolds come with a risk for protein structural stability, and some scaffold variants were even shown to destabilize the transition state.[41,42]

Here, we present an alternative to scaffold modification for improving synthetic enzymes that relies on modifying the surrounding environment. Indeed, since catalysis is governed by both short-range and long-range electrostatic interactions within the electrostatic preorganization theory,[43] it should be possible to introduce external factors around the protein that will play the role of a functional scaffold without the inconveniences of scaffold modification (i.e., disruption of protein structural stability, local unfolding, etc.). Modifying the greater environment, rather than the protein scaffold, has the added benefit of simplifying the adaptation of synthetic enzymes to the broad range of industrial operating conditions, because it does not require new protein structures to be designed for each case.
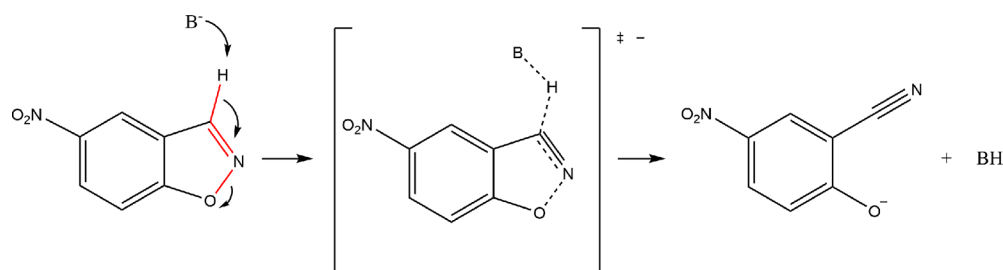
Using the fundamental principles of electrostatic preorganization, we can infer that any polar molecular component could

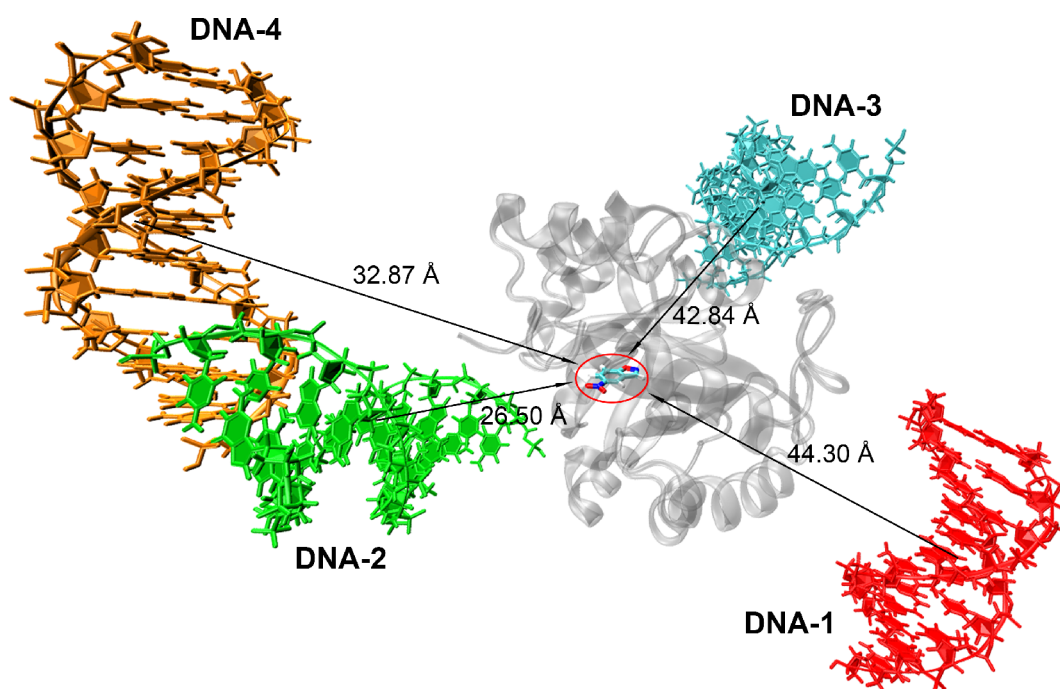**Figure 1.** Reaction mechanism of Kemp elimination. The 5-benzisoxazole ring is deprotonated by a catalytic base, leading to the ring opening by breaking the C−H and O−N bonds and the formation of the C−N triple bond. The breakage and formation of the bonds are colored in red.

Figure 2. Double-helix DNA fragment (10 bases long) is placed at different positions around KE15. The four KE15−DNA systems considered in this study are represented with different colors. The ligand is shown in the middle of the protein scaffold (1THF barrel scaffold) in the red circle. The distance between the DNA fragment and the ligand is labeled.

induce long-range electrostatic interactions that would stabilize the transition state in the active site. However, from a design perspective, we would like the structure and orientation of this molecular component to be easily controlled. In this paper, we choose to introduce DNA in the environment of the enzyme, because its high programmability from predictable base-pair interactions facilitates custom structural designs, as DNA origamis examplify.[44−47] Further, many noncovalent and covalent conjugation methods with proteins have been developed in the context of protein networks, which suggests that DNA does not threaten protein structural stability or enzymatic activity.[48−53]

Here, we present a series of computational experiments that demonstrate that the highly polar sugar−phosphate backbone of DNA can induce long-range electrostatic interactions that increase the catalytic rate of Kemp eliminase KE15. Previous work on KE15 clearly demonstrated the scaffold's inability to support the reaction in the active site,[54,55] making it the ideal candidate for this study. Meanwhile the Kemp elimination reaction, shown in Figure 1, offers mechanistic simplicity with a one-step mechanism.[54,56]

To demonstrate our DNA-based performance enhancement strategy, we randomly selected four different positions around KE15 (Figure 2) to place a double-helix DNA fragment (10 bases long) and quantified its effect on the stabilization of the transition state. We find that one of these four positions lower the activation energy by 2.0 kcal/mol, suggesting that further optimization of DNA structure (including tethering to the protein) and orientation could have a tremendous benefit on catalysis.

■ METHODS

Conformational Ensemble. We generated 25 different structures for each system (the four DNA−KE15 systems) and each state (reactant and transition state) as follows. The 25 structures were created from a backbone conformational search and side-chain ensemble simulation. We used the backrub algorithm[57,58] from the ROSETTA package to generate 25 uncorrelated low energy backbone conformations from $25 \times 10\,000$ trials. The backrub algorithm rotates the protein backbone as a static body about the α carbon, C_α.[58] We then repacked the side chains for the 25 low energy backbone structures, using the fixbb algorithm from
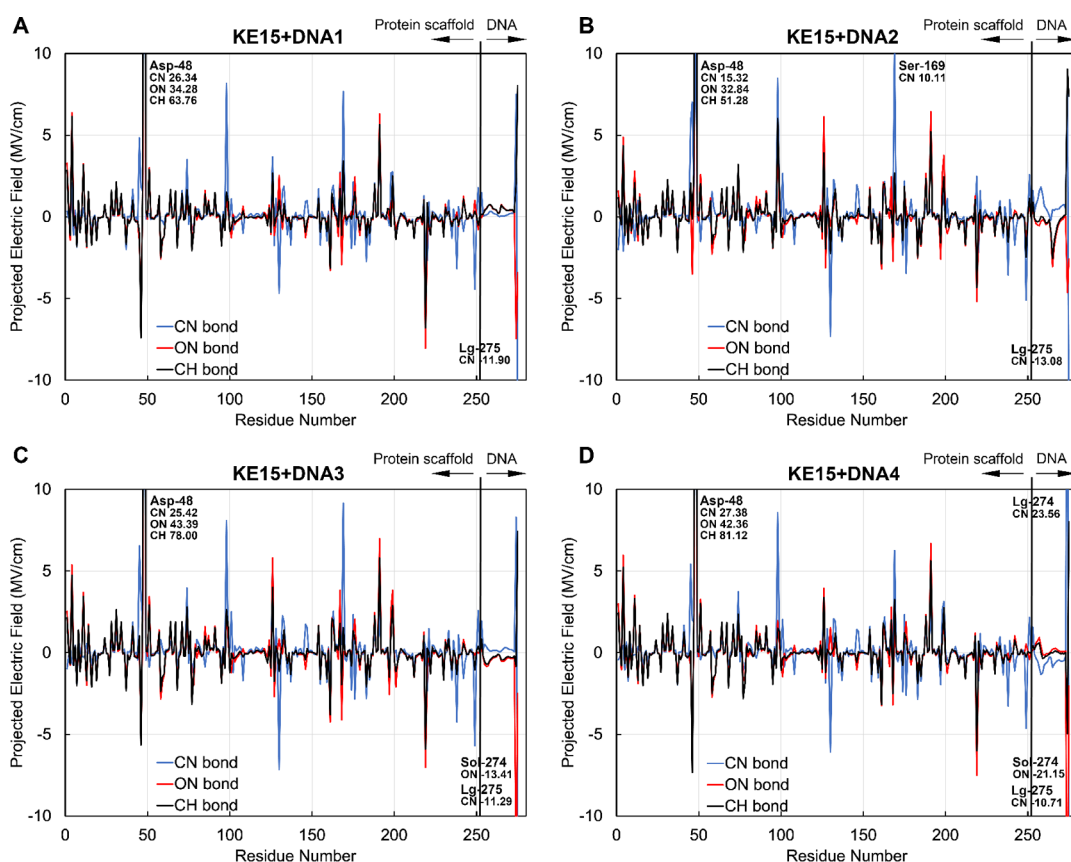
Figure 3. Contribution of an individual residue to the transition state electric field of four different DNA positions, (A−D). Projections onto the C−N, O−N, and C−H bonds are shown in blue, red, and black, respectively. Contribution peaks higher than 10 MV/cm are cut off the graph and labeled on the side of the peak, for clarity. Residues 1 to 253 correspond to the KE15 protein scaffold, residue 48 being the catalytic base. The DNA fragment starts from residue 254 and ends at residue 273. Residue 274 represents the solvent (water and counterions), and residue 275 is the ligand.

ROSETTA. Fixbb is a Monte Carlo method that samples the Dunbrack backbone-dependent rotamer library.[59] As a result, these 25 structures make a conformational ensemble that spans the time scale required to pivot the backbone along the α carbons and switch side-chain rotamers. NMR J-coupling experiments have quantified that such side-chain conformational transitions occur on time scales of nanoseconds to microseconds.[60−63]

We then used PACKMOL[64] to place the DNA double-helix fragment (GGTCATGACC−CCAGTACTGG) around the enzyme and determine the periodic boundary conditions for each protein, with a 10 Å buffer on each side. This results in solvent boxes of sizes $80 \times 106 \times 72$ Å^3 for KE15+DNA1, $86 \times 97 \times 79$ Å^3 for KE15+DNA2, $103 \times 97 \times 89$ Å^3 for KE15+DNA3, and $86 \times 88 \times 87$ Å^3 for KE15+DNA4. The starting KE15−DNA structures are available on our group's Github at https://github.com/WelbornGroup/.

Molecular Dynamics. We performed molecular dynamic (MD) simulations in Tinker[65] for all four DNA−KE15 systems (reactant state and transition state) using the AMOEBA polarizable force field[66,67] under constant pressure (1 atm) and temperature (300 K) and with a 1 fs time step for 100 ps (including 50 ps of equilibration). All systems were solvated with a pre-equilibrated water solvent box using GROMACS's algorithm solvate,[68−70] which accelerated the equilibration process (see convergence data in the Supporting Information). After equilibration, data was collected every 1 ps for 50 ps for each of the structures. With 25 structures per state, this adds to

a total of 1.25 ns of production data, seeded from a conformational ensemble that describes nanosecond to microsecond time scales, from which we can calculate catalytic properties. The transition state was modeled using the geometry of the reactant state but assigning partial charges to atoms that reflect the transition state charge density, as described in ref 55. The input and parameter files are also available in our group's Github.

Electrostatic Stabilization of the Transition State. The electrostatic stabilization of the transition state was calculated as

$$\Delta G_{elec}^{\ddagger} = -\sum_{\text{active bonds}} (\overline{\mu}_{EL}^{\ddagger}\overline{E}_{EL}^{\ddagger} - \overline{\mu}_{EL}\overline{E}_{EL}) \qquad (1)$$

where $\overline{\mu}_{EL}$ and $\overline{E}_{EL}$ represent the active bond dipole moment and the electric field respectively, and $\ddagger$ indicates the transition state. In this case, we focus on three active bonds: the C−H, C−N, and O−N bonds as highlighted in Figure 1. The corresponding bond dipoles for both the reactant and the transition state were taken from ref 55 and given in the Supporting Information. We calculated the electric fields projected onto a user-defined bond as

$$E_{proj}^{ij} = \frac{(\vec{E}^i + \vec{E}^j)}{2} \cdot \vec{u}^{ij} \qquad (2)$$

where E_{proj}^{ij} is the electric field projected onto bond ij, $\vec{u}^{ij}$ is the unitary vector defining bond ij, and $\vec{E}^i$ is the field at atom i.[71]

Table 1. Stabilization Free Energy of the Transition State for Each KE15–DNA System[a]

		$\Delta G_{elec}^{\ddagger}$ (kcal/mol)					
bond	system	base	active site	scaffold	DNA	solvent	total
C–H	KE15[55]	−4.6	0.1	−1.0	N/A	0.1	−5.4
	KE15+DNA1	−5.1 ± 0.05	0.1 ± 0.03	−0.4 ± 0.06	−0.8 ± 0.001	0.1 ± 0.04	−6.1 ± 0.09
	KE15+DNA2	−4.9 ± 0.06	−0.3 ± 0.02	−1.0 ± 0.07	1.1 ± 0.004	−0.3 ± 0.03	−5.4 ± 0.1
	KE15+DNA3	−7.1 ± 0.07	0.2 ± 0.03	−0.5 ± 0.08	0.7 ± 0.001	0.5 ± 0.03	−6.2 ± 0.1
	KE15+DNA4	−5.9 ± 0.06	0.6 ± 0.03	−0.5 ± 0.07	−0.4 ± 0.002	0.6 ± 0.04	−5.6 ± 0.1
O–N	KE15[55]	−6.0	1.1	−1.6	N/A	3.2	−3.3
	KE15+DNA1	−5.6 ± 0.04	1.2 ± 0.05	−0.3 ± 0.08	−1.5 ± 0.002	2.0 ± 0.05	−4.2 ± 0.1
	KE15+DNA2	−5.9 ± 0.05	0.1 ± 0.05	−1.4 ± 0.07	2.7 ± 0.007	1.2 ± 0.05	−3.3 ± 0.1
	KE15+DNA3	−7.7 ± 0.05	1.2 ± 0.05	−0.7 ± 0.08	1.7 ± 0.003	2.8 ± 0.06	−2.7 ± 0.1
	KE15+DNA4	−6.8 ± 0.05	1.4 ± 0.05	−0.7 ± 0.07	−1.2 ± 0.005	4.3 ± 0.06	−3.0 ± 0.1
C–N	KE15[55]	2.0	0.0	0.8	N/A	0.2	−3.0
	KE15+DNA1	1.1 ± 0.03	0.4 ± 0.04	1.0 ± 0.06	0.3 ± 0.002	−0.2 ± 0.04	2.6 ± 0.09
	KE15+DNA2	1.7 ± 0.04	0.7 ± 0.03	0.9 ± 0.06	0.4 ± 0.005	−0.7 ± 0.04	3.0 ± 0.08
	KE15+DNA3	2.3 ± 0.05	0.6 ± 0.04	1.1 ± 0.07	−0.1 ± 0.004	−0.9 ± 0.04	3.0 ± 0.1
	KE15+DNA4	1.4 ± 0.03	0.4 ± 0.03	1.4 ± 0.06	−0.5 ± 0.004	−0.2 ± 0.05	2.5 ± 0.09
total	KE15[55]	−8.6	1.2	−1.8	N/A	3.5	−5.7
	KE15+DNA1	−9.6 ± 0.07	1.7 ± 0.08	0.3 ± 0.11	−2.0 ± 0.002	1.9 ± 0.08	−7.7 ± 0.17
	KE15+DNA2	−9.1 ± 0.09	0.5 ± 0.06	−1.5 ± 0.11	4.2 ± 0.01	0.2 ± 0.07	−5.7 ± 0.17
	KE15+DNA3	−12.5 ± 0.10	2.0 ± 0.07	−0.1 ± 0.13	2.3 ± 0.004	2.4 ± 0.08	−5.9 ± 0.20
	KE15+DNA4	−11.3 ± 0.08	2.4 ± 0.06	0.2 ± 0.11	−2.1 ± 0.006	4.7 ± 0.09	−6.1 ± 0.18

[a]$\Delta G_{elec}^{\ddagger}$ for KE15 without a DNA fragment is from ref 55. The active site includes residues 5, 46, 78, 101, 126, 167, 168, 169, 197, 198, 199, 201, and 220 (+ base), and the solvent includes water and the counterion Na⁺. The error is calculated as the error of the mean from our time and ensemble averages.

The x-component of the electric field at each atom site is defined as

$$E_x^i = \sum_j \left(E_{x,perm}^{j \to i} + E_{x,ind}^{j \to i} \right)$$

(3)

accounting for both permanent (perm) and induced (ind) fields.[71]

The electrostatic stabilization energy of the transition state was calculated according to eq 1, where the bond dipole moment $\bar{\mu}_{EL}$ was obtained from ref 55.

The electric fields were calculated for the three bonds that break and form during the reaction (see Figure 1), using the ELECTRIC code published open-source.[71]

Note that the computational protocol described here follows the protocol described in refs 22, 55, 61, and 72.

RESULTS AND DISCUSSION

Figure 3 shows the contribution of each protein residue, DNA base, and solvent to the electric fields in the active site of KE15, calculated in the transition state. We consider the projection of these fields onto three bonds, namely C–H, C–N, and O–N. Note that these three bonds form a set of active bonds, from which other bonds involved in the reaction can be described. For example, the formation of the Asp-48–H bond is complementary to the breaking of the C–H bond.

Comparing these plots with a previously published plot for the KE15 design (i.e., without DNA),[55] we can make two observations. First, the overall contributions from the protein residues follow a similar trend with or without DNA. This means that the DNA fragments do not induce new interactions between the protein and the ligand in the active site. Rather, the DNA fragments exacerbate existing interactions. For example, the catalytic base, Asp-48, remains the only contribution over 10 MV/cm, but its magnitude is increased by 65% for the formation of the C–H bond, 296% for the

formation of the C–N bond, and 21% for the breaking of the O–N bond (DNA4). Similar conclusions can be reached looking at the contributions of the top contributors, Asp-98, Ser-169, and Asp-219. Interestingly, while Ser-169 is located in the active site, Asp-98 and Asp-219 are close to the surface of the scaffold. This means that our DNA fragments can enhance contributions of residues throughout the protein structure, for an overall net benefit on catalysis.

The second observation is that individual DNA bases, regardless of position, do not seem to directly contribute to the electric fields in the active site (i.e., the peaks for residues 254 to 273 are negligible). However, there is a noticeable difference in the total field when comparing our KE15+DNA systems to our reference system (KE15 without a DNA fragment). This would suggest that the effect of DNA fragments is delivered indirectly, through the solvent and protein scaffold whose electric field contribution has changed across the systems. To better analyze the overall effect of the DNA fragments on KE15 catalytic activity, we present calculations of the stabilization free energy of the transition state, $\Delta G_{elec}^{\ddagger}$, in Table 1.

In Table 1, we see that two of the DNA fragments, DNA1 and DNA4, directly contribute 2.0 kcal/mol to the stabilization of the transition state. Considering the 4.0–6.0 kcal/mol difference with the contribution of DNA2 and DNA3 (of identical sequence), we envision significant control of the catalytic activity via the sole positioning of DNA fragments around the enzyme.

However, the largest increase in transition state stabilization free energy comes from the contribution of the base, consistent with our analysis of the projected electric fields in the transition state. Meanwhile, the additive effects on the active site and scaffold are minimal and tend to equally stabilize and destabilize the transition state, compared to the KE15 design. Finally, we note that DNA1–3 also induced a significant

solvent contribution to $\Delta G_{elec}{}^{\ddagger}$. More specifically, it seems that part of the effect of DNA1−3 is to displace "bad" catalytic waters, replacing them with a DNA fragment that induces favorable stabilization of the transition state in the active site. This is consistent with the finding in a previous study by Acosta-Silva et al., who have shown that polar aprotic solvent can largely increase the reaction rate of the Kemp elimination reaction.[73]

Overall, the introduction of a DNA fragment had either no effect (DNA2 and DNA3) or further stabilized the transition state compared to KE15 design (DNA1 and DNA4). Remarkably, KE15+DNA1 exhibited a 2.0 kcal/mol difference in the total activation energy, which corresponds to a 30-fold increase in the kinetic rate at ambient temperature. Considering that DNA1 and DNA3 are further away from the ligand, these results suggest that the DNA fragment needs not to be placed in the immediate vicinity of the ligand, offering valuable structural flexibility for design. For a fixed DNA sequence, it seems that the orientation of the DNA fragment with respect to the enzyme has a larger effect on the stabilization free energy than the protein−DNA distance.

CONCLUSIONS

In summary, the data presented here demonstrate that a DNA fragment in the surroundings of KE15 can be used to tune the catalytic activity of the enzyme. Part of this effect is delivered through the solvent, enhancing the contributions of residues at the protein surface. Although the orientation of the DNA fragment relative to the enzyme plays a major role, we were able to reach a 2.0 kcal/mol difference in the transition state stabilization energy in one of our four test systems. This is particularly notable, because our systems were designed for a demonstration of a principle where the DNA orientation was randomly chosen, and the DNA size or sequence were not optimized. This suggests that significant activity improvements could be achieved via a systematic design of DNA size, sequence, and positioning. Further work involves investigating the role on catalysis of larger DNA structures, such as DNA origamis whose synthesis and binding to proteins are already established and can be controlled.[74−76]

ASSOCIATED CONTENT

Ⓢ Supporting Information

The Supporting Information is available free of charge at https://pubs.acs.org/doi/10.1021/acs.jpcb.2c00765.

> Table S1: Active bond dipole moments; Figures S1−S4: MD energy convergence plots for protein−DNA complexes; Figures S5−S8: RMSD plots for protein−DNA complexes (PDF)

AUTHOR INFORMATION

Corresponding Author
   Valerie Vaissier Welborn − *Department of Chemistry, Virginia Tech, Blacksburg, Virginia 24060, United States;* Ⓞ orcid.org/0000-0003-0834-4441; Email: vwelborn@vt.edu

Author
   Yi Zheng − *Department of Chemistry, Virginia Tech, Blacksburg, Virginia 24060, United States*

Complete contact information is available at:
https://pubs.acs.org/10.1021/acs.jpcb.2c00765

Notes
The authors declare no competing financial interest.

REFERENCES

(1) Bommarius, A. S.; Paye, M. F. Stabilizing Biocatalysts. *Chem. Soc. Rev.* **2013**, *42*, 6534.

(2) Chapman, J.; Ismail, A.; Dinu, C. Industrial Applications of Enzymes: Recent Advances, Techniques, and Outlooks. *Catalysts* **2018**, *8*, 238.

(3) Singh, R.; Kumar, M.; Mittal, A.; Mehta, P. K. Microbial Enzymes: Industrial Progress in 21st Century. *3 Biotech* **2016**, *6*, 174.

(4) Steiner, K.; Schwab, H. Recent Advances in Rational Approaches For Enzyme Engeineering. *Comput. Struct. Biotechnol. J.* **2012**, *2*, No. e201209010.

(5) Currin, A.; Swainston, N.; Day, P. J.; Kell, D. B. Synthetic Biology for the Directed Evolution of Protein Biocatalysts: Navigating Sequence Space Intelligently. *Chem. Soc. Rev.* **2015**, *44*, 1172−1239.

(6) Jeschek, M.; Reuter, R.; Heinisch, T.; Trindler, C.; Klehr, J.; Panke, S.; Ward, T. R. Directed Evolution of Artificial Metalloenzymes for in Vivo Metathesis. *Nature* **2016**, *537*, 661−665.

(7) Nanda, V.; Koder, R. L. Designing Artificial Enzymes by Intuition and Computation. *Nat. Chem.* **2010**, *2*, 15−24.

(8) Ward, T. Artificial Enzymes Made to Order: Combination of Computational Design and Directed Evolution. *Angew. Chem., Int. Ed. Engl.* **2008**, *47*, 7802−7803.

(9) Nixon, A. E.; Firestine, S. M.; Salinas, F. G.; Benkovic, S. J. Rational Design of a Scytalone Dehydratase-Like Enzyme Using a Structurally Homologous Protein Scaffold. *Proc. Natl. Acad. Sci. U. S. A.* **1999**, *96*, 3568−3571.

(10) Araki, M.; Okuno, Y.; Hara, Y.; Sugiura, Y. Allosteric Regulation of a Ribozyme Activity Through Ligand-Induced Conformational Change. *Nucleic Acids Res.* **1998**, *26*, 3379−3384.

(11) Korendovych, I. V.; DeGrado, W. F. Catalytic Efficiency of Designed Catalytic Proteins. *Curr. Opin. Struct. Biol.* **2014**, *27*, 113−121.

(12) Preiswerk, N.; Beck, T.; Schulz, J. D.; Milovnik, P.; Mayer, C.; Siegel, J. B.; Baker, D.; Hilvert, D. Impact of Scaffold Rigidity on the Design and Evolution of an Artificial Diels-Alderase. *Proc. Natl. Acad. Sci. U. S. A.* **2014**, *111*, 8013−8018.

(13) Kiss, G.; Çelebi-Ölçüm, N.; Moretti, R.; Baker, D.; Houk, K. N. Computational Enzyme Design. *Angew. Chem., Int. Ed. Engl.* **2013**, *52*, 5700−5725.

(14) Rothlisberger, D.; Khersonsky, O.; Wollacott, A. M.; Jiang, L.; DeChancie, J.; Betker, J.; Gallaher, J. L.; Althoff, E. A.; Zanghellini, A.; Dym, O.; Albeck, S.; Houk, K. N.; Tawfik, D. S.; Baker, D. Kemp Elimination Catalysts by Computational Enzyme Design. *Nature* **2008**, *453*, 190−195.

(15) Khersonsky, O.; Kiss, G.; Rothlisberger, D.; Dym, O.; Albeck, S.; Houk, K. N.; Baker, D.; Tawfik, D. S. Bridging the Gaps in Design Methodologies by Evolutionary Optimization of the Stability and Proficiency of Designed Kemp Eliminase KE59. *Proc. Natl. Acad. Sci. U. S. A.* **2012**, *109*, 10358−10363.

(16) Khersonsky, O.; Röthlisberger, D.; Wollacott, A. M.; Murphy, P.; Dym, O.; Albeck, S.; Kiss, G.; Houk, K.; Baker, D.; Tawfik, D. S. Optimization of the In-Silico-Designed Kemp Eliminase KE70 by Computational Design and Directed Evolution. *J. Mol. Biol.* **2011**, *407*, 391−412.

(17) Frushicheva, M. P.; Cao, J.; Chu, Z. T.; Warshel, A. Exploring Challenges in Rational Enzyme Design by Simulating the Catalysis in Artificial Kemp Eliminase. *Proc. Natl. Acad. Sci. U. S. A.* **2010**, *107*, 16869−16874.

(18) Korendovych, I. V.; Kulp, D. W.; Wu, Y.; Cheng, H.; Roder, H.; DeGrado, W. F. Design of a Switchable Eliminase. *Proc. Natl. Acad. Sci. U. S. A.* **2011**, *108*, 6823−6827.

(19) Privett, H. K.; Kiss, G.; Lee, T. M.; Blomberg, R.; Chica, R. A.; Thomas, L. M.; Hilvert, D.; Houk, K. N.; Mayo, S. L. Iterative Approach to Computational Enzyme Design. *Proc. Natl. Acad. Sci. U. S. A.* **2012**, *109*, 3790−3795.

(20) Tantillo, D. J.; Jiangang, C.; Houk, K. N. Theozymes and Compuzymes: Theoretical Models for Biological Catalysis. *Curr. Opin. Chem. Biol.* **1998**, *2*, 743−750.

(21) Tantillo, D. J.; Houk, K. N. Theozymes and Catalyst Design. *Stimulating Concepts in Chemistry* **2005**, 79−88.

(22) Vaissier Welborn, V.; Head-Gordon, T. Computational Design of Synthetic Enzymes. *Chem. Rev.* **2019**, *119*, 6613−6630.

(23) Robinson, P. K. Enzymes: Principles and Biotechnological Applications. *Essays Biochem* **2015**, *59*, 1−41.

(24) Warshel, A.; Sharma, P. K.; Kato, M.; Xiang, Y.; Liu, H.; Olsson, M. H. M. Electrostatic Basis for Enzyme Catalysis. *Chem. Rev.* **2006**, *106*, 3210−3235.

(25) Lechner, H.; Ferruz, N.; Höcker, B. Strategies for Designing Non-Natural Enzymes and Binders. *Curr. Opin. Chem. Biol.* **2018**, *47*, 67−76.

(26) Świderek, K.; Tuñón, I.; Moliner, V.; Bertran, J. Computational Strategies for the Design of New Enzymatic Functions. *Arch. Biochem. Biophys.* **2015**, *582*, 68−79.

(27) Fazelinia, H.; Cirino, P. C.; Maranas, C. D. OptGraft: A Computational Procedure for Transferring a Binding Site onto an Existing Protein Scaffold. *Protein Sci.* **2008**, 180−195.

(28) Malisi, C.; Kohlbacher, O.; Höcker, B. Automated Scaffold Selection for Enzyme Design. *Proteins* **2009**, *77*, 74−83.

(29) Huang, X.; Han, K.; Zhu, Y. Systematic Optimization Model and Algorithm for Binding Sequence Selection in Computational Enzyme Design. *Protein Sci.* **2013**, *22*, 929−941.

(30) Nosrati, G. R.; Houk, K. N. SABER: A Computational Method for Identifying Active Sites for New Reactions. *Protein Sci.* **2012**, *21*, 697−706.

(31) Oh, K.; Yi, G.-S. Prediction of Scaffold Proteins Based on Protein Interaction and Domain Architectures. *BMC Bioinf* **2016**, *17*, 220.

(32) Alexandrova, A. N.; Röthlisberger, D.; Baker, D.; Jorgensen, W. L. Catalytic Mechanism and Performance of Computationally Designed Enzymes for Kemp Elimination. *J. Am. Chem. Soc.* **2008**, *130*, 15907−15915.

(33) Brustad, E. M.; Arnold, F. H. Optimizing Non-Natural Protein Function with Directed Evolution. *Curr. Opin. Chem. Biol.* **2011**, *15*, 201−210.

(34) Dalby, P. A. Strategy and Success for the Directed Evolution of Enzymes. *Curr. Opin. Struct. Biol.* **2011**, *21*, 473−480.

(35) Hong, N.-S.; Petrović, D.; Lee, R.; Gryn'ova, G.; Purg, M.; Saunders, J.; Bauer, P.; Carr, P. D.; Lin, C.-Y.; Mabbitt, P. D.; et al. The Evolution of Multiple Active Site Configurations in a Designed Enzyme. *Nat. Commun.* **2018**, *9*, 3900.

(36) Li, A.; Wang, B.; Ilie, A.; Dubey, K. D.; Bange, G.; Korendovych, I. V.; Shaik, S.; Reetz, M. T. A Redox-Mediated Kemp Eliminase. *Nat. Commun.* **2017**, *8*, 14876.

(37) Voigt, C. A.; Mayo, S. L.; Arnold, F. H.; Wang, Z.-G. Computational Method to Reduce the Search Space for Directed Protein Evolution. *Proc. Natl. Acad. Sci. U. S. A.* **2001**, *98*, 3778−3783.

(38) Turner, N. J. Directed Evolution Drives the Next Generation of Biocatalysts. *Nat. Chem. Biol.* **2009**, *5*, 567−573.

(39) Dunn, M. R.; Otto, C.; Fenton, K. E.; Chaput, J. C. Improving Polymerase Activity with Unnatural Substrates by Sampling Mutations in Homologous Protein Architectures. *ACS Chem. Biol.* **2016**, *11*, 1210−1219.

(40) Park, H.-S.; Nam, S.-H.; Lee, J. K.; Yoon, C. N.; Mannervik, B.; Benkovic, S. J.; Kim, H.-S. Design and Evolution of New Catalytic Activity with an Existing Protein Scaffold. *Science* **2006**, *311*, 535−538.

(41) Claren, J.; Malisi, C.; Hocker, B.; Sterner, R. Establishing Wild-Type Levels of Catalytic Activity on Natural and Artificial $(\beta\alpha)_8$-Barrel Protein Scaffolds. *Proc. Natl. Acad. Sci. U. S. A.* **2009**, *106*, 3704−3709.

(42) Tokuriki, N.; Stricher, F.; Serrano, L.; Tawfik, D. S. How Protein Stability and New Functions Trade Off. *PLoS Comput. Biol.* **2008**, *4*, No. e1000002.

(43) Warshel, A.; Sharma, P. K.; Kato, M.; Xiang, Y.; Liu, H.; Olsson, M. H. M. Electrostatic Basis for Enzyme Catalysis. *Chem. Rev.* **2006**, *106*, 3210−3235.

(44) Kurita, N.; Danilov, V. I.; Anisimov, V. M. The Structure of Watson−Crick DNA Base Pairs Obtained by MP2 Optimization. *Chem. Phys. Lett.* **2005**, *404*, 164−170.

(45) Saenger, W.; Hunter, W. N.; Kennard, O. DNA Conformation is Determined by Economics in the Hydration of Phosphate Groups. *Nature* **1986**, *324*, 385−388.

(46) Patel, D.; Pardi, A.; Itakura, K. DNA Conformation, Dynamics, and Interactions in Solution. *Science* **1982**, *216*, 581−590.

(47) Pinheiro, A. V.; Han, D.; Shih, W. M.; Yan, H. Challenges and Opportunities for Structural DNA Nanotechnology. *Nat. Nanotechnol.* **2011**, *6*, 763−772.

(48) Rosen, C. B.; Kodal, A. L. B.; Nielsen, J. S.; Schaffert, D. H.; Scavenius, C.; Okholm, A. H.; Voigt, N. V.; Enghild, J. J.; Kjems, J.; Tørring, T.; et al. Template-Directed Covalent Conjugation of DNA to Native Antibodies, Transferrin and Other Metal-Binding Proteins. *Nat. Chem.* **2014**, *6*, 804−809.

(49) Trads, J. B.; Tørring, T.; Gothelf, K. V. Site-Selective Conjugation of Native Proteins with DNA. *Acc. Chem. Res.* **2017**, *50*, 1367−1374.

(50) Li, S.; Gao, Z.; Shao, N. Non-Covalent Conjugation of CdTe QDs with Lysozyme Binding DNA for Fluorescent Sensing of Lysozyme in Complex Biological Sample. *Talanta* **2014**, *129*, 86−92.

(51) Yang, Y. R.; Liu, Y.; Yan, H. DNA Nanostructures as Programmable Biomolecular Scaffolds. *Bioconjugate Chem.* **2015**, *26*, 1381−1395.

(52) Niemeyer, C. Semisynthetic DNA-Protein Conjugates for Biosensing and Nanofabrication. *Angew. Chem., Int. Ed. Engl.* **2010**, *49*, 1200−1216.

(53) Goodman, R. P.; Erben, C. M.; Malo, J.; Ho, W. M.; McKee, M. L.; Kapanidis, A. N.; Turberfield, A. J. A Facile Method for Reversibly Linking a Recombinant Protein to DNA. *ChemBioChem.* **2009**, *10*, 1551−1557.

(54) Lamba, V.; Sanchez, E.; Fanning, L. R.; Howe, K.; Alvarez, M. A.; Herschlag, D.; Forconi, M. Kemp Eliminase Activity of Ketosteroid Isomerase. *Biochemistry* **2017**, *56*, 582−591.

(55) Vaissier, V.; Sharma, S. C.; Schaettle, K.; Zhang, T.; Head-Gordon, T. Computational Optimization of Electric Fields for Improving Catalysis of a Designed Kemp Eliminase. *ACS Catal.* **2018**, *8*, 219−227.

(56) Casey, M. L.; Kemp, D. S.; Paul, K. G.; Cox, D. D. Physical Organic Chemistry of Benzisoxazoles. I. Mechanism of the Base-Catalyzed Decomposition of Benzisoxazoles. *J. Org. Chem.* **1973**, *38*, 2294−2301.

(57) Davis, I. W.; Arendall, W. B., III; Richardson, D. C.; Richardson, J. S. The Backrub Motion: How Protein Backbone Shrugs When a Sidechain Dances. *Structure* **2006**, *14*, 265−274.

(58) Smith, C. A.; Kortemme, T. Backrub-Like Backbone Simulation Recapitulates Natural Protein Conformational Variability and Improves Mutant Side-Chain Prediction. *J. Mol. Biol.* **2008**, *380*, 742−756.

(59) Shapovalov, M. V.; Dunbrack, R. L., Jr A Smoothed Backbone-Dependent Rotamer Library for Proteins Derived from Adaptive Kernel Density Estimates and Regressions. *Structure* **2011**, *19*, 844−858.

(60) Chou, J. J.; Case, D. A.; Bax, A. Insights into the Mobility of Methyl-Bearing Side Chains in Proteins from 3 J CC and 3 J CN Couplings. *J. Am. Chem. Soc.* **2003**, *125*, 8959−8966.

(61) Welborn, V. V.; Head-Gordon, T. Fluctuations of Electric Fields in the Active Site of the Enzyme Ketosteroid Isomerase. *J. Am. Chem. Soc.* **2019**, *141*, 12487−12492.

(62) Keedy, D. A.; Kenner, L. R.; Warkentin, M.; Woldeyes, R. A.; Hopkins, J. B.; Thompson, M. C.; Brewster, A. S.; Van Benschoten, A. H.; Baxter, E. L.; Uervirojnangkoorn, M.; et al. Mapping the Conformational Landscape of a Dynamic Enzyme by Multitemperature and XFEL Crystallography. *Elife* **2015**, *4*, No. e07574.

(63) Smith, C. A.; Ban, D.; Pratihar, S.; Giller, K.; Schwiegk, C.; de Groot, B. L.; Becker, S.; Griesinger, C.; Lee, D. Population Shuffling of Protein Conformations. *Angew. Chem., Int. Ed. Engl.* **2015**, *54*, 207−210.

(64) Martínez, L.; Andrade, R.; Birgin, E. G.; Martínez, J. M. PACKMOL: a Package for Building Initial Configurations for Molecular Dynamics Simulations. *J. Comput. Chem.* **2009**, *30*, 2157−2164.

(65) Rackers, J. A.; Wang, Z.; Lu, C.; Laury, M. L.; Lagardère, L.; Schnieders, M. J.; Piquemal, J.-P.; Ren, P.; Ponder, J. W. Tinker 8: Software Tools for Molecular Design. *J. Chem. Theory Comput.* **2018**, *14*, 5273−5289.

(66) Zhang, C.; Lu, C.; Jing, Z.; Wu, C.; Piquemal, J.-P.; Ponder, J. W.; Ren, P. AMOEBA Polarizable Atomic Multipole Force Field for Nucleic Acids. *J. Chem. Theory Comput.* **2018**, *14*, 2084−2108.

(67) Shi, Y.; Xia, Z.; Zhang, J.; Best, R.; Wu, C.; Ponder, J. W.; Ren, P. Polarizable Atomic Multipole-Based AMOEBA Force Field for Proteins. *J. Chem. Theory Comput.* **2013**, *9*, 4046−4063.

(68) Pronk, S.; Páll, S.; Schulz, R.; Larsson, P.; Bjelkmar, P.; Apostolov, R.; Shirts, M. R.; Smith, J. C.; Kasson, P. M.; van der Spoel, D.; et al. GROMACS 4.5: a High-Throughput and Highly Parallel Open Source Molecular Simulation Toolkit. *Bioinformatics* **2013**, *29*, 845−854.

(69) Páll, S.; Abraham, M. J.; Kutzner, C.; Hess, B.; Lindahl, E. Tackling Exascale Software Challenges in Molecular Dynamics Simulations with GROMACS. *Solving Software Challenges for Exascale* **2015**, *8759*, 3−27.

(70) Abraham, M. J.; Murtola, T.; Schulz, R.; Páll, S.; Smith, J. C.; Hess, B.; Lindahl, E. GROMACS: High Performance Molecular Simulations through Multi-Level Parallelism from Laptops to Supercomputers. *SoftwareX* **2015**, *1−2*, 19−25.

(71) Nash, J.; Barnes, T.; Welborn, V. ELECTRIC: Electric fields Leveraged from Multipole Expansion Calculations in Tinker Rapid Interface Code. *J. Open Source Softw.* **2020**, *5*, 2576.

(72) Lawal, M. M.; Vaissier Welborn, V. Structural Dynamics Support Electrostatic Interactions in the Active Site of Adenylate Kinase. *ChemBioChem.* **2022**, e202200097.

(73) Acosta-Silva, C.; Bertran, J.; Branchadell, V.; Oliva, A. Kemp Elimination Reaction Catalyzed by Electric Fields. *ChemPhysChem* **2020**, *21*, 295−306.

(74) Douglas, S. M.; Bachelet, I.; Church, G. M. A Logic-Gated Nanorobot for Targeted Transport of Molecular Payloads. *Science* **2012**, *335*, 831−834.

(75) Schüller, V. J.; Heidegger, S.; Sandholzer, N.; Nickels, P. C.; Suhartha, N. A.; Endres, S.; Bourquin, C.; Liedl, T. Cellular Immunostimulation by CpG-Sequence-Coated DNA Origami Structures. *ACS Nano* **2011**, *5*, 9696−9702.

(76) Elbaz, J.; Yin, P.; Voigt, C. A. Genetic Encoding of DNA Nanostructures and Their Self-Assembly in Living Bacteria. *Nat. Commun.* **2016**, *7*, 11179.

🔲 Recommended by ACS

Local Electric Fields: From Enzyme Catalysis to Synthetic Catalyst Design

Kshatresh Dutta Dubey, Sason Shaik, *et al.*

DECEMBER 05, 2022
THE JOURNAL OF PHYSICAL CHEMISTRY B　　　　READ ☑

Computer Simulations Reveal an Entirely Entropic Activation Barrier for the Chemical Step in a Designer Enzyme

Johan Åqvist.

JANUARY 10, 2022
ACS CATALYSIS　　　　READ ☑

Tuning Enzyme Thermostability via Computationally Guided Covalent Stapling and Structural Basis of Enhanced Stabilization

Jacob A. Iannuzzelli, Rudi Fasan, *et al.*

MAY 25, 2022
BIOCHEMISTRY　　　　READ ☑

Energetic Basis and Design of Enzyme Function Demonstrated Using GFP, an Excited-State Enzyme

Chi-Yun Lin, Steven G. Boxer, *et al.*

FEBRUARY 24, 2022
JOURNAL OF THE AMERICAN CHEMICAL SOCIETY　　　　READ ☑

Get More Suggestions >